

The methane mono-oxygenase reaction system studied *in vivo* by membrane-inlet mass spectrometry

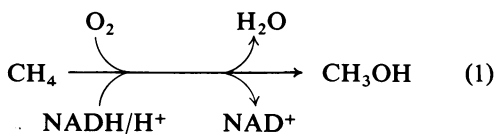
Lars JOERGENSEN

Institute of Biochemistry, Odense University, DK-5230 Odense M, Denmark

(Received 23 July 1984/Accepted 1 October 1984)

A membrane-inlet mass spectrometer connected to an open-system cuvette was used for direct measurement of dissolved methane and O₂ in bacterial samples of strain OU-4-1, a type II methanotrophic bacterium. A technique was applied for keeping the concentration of dissolved methane or O₂ in the sample constant while the concentration of the other dissolved gas was varied. This allowed the reaction mechanism of methane mono-oxygenase to be studied *in vivo*. The enzyme was found to follow a random bi-reactant mechanism with respect to binding of methane and O₂. Binding of one substrate decreased the affinity for the other. The true binding constants were 1 μM for methane and 0.14 μM for O₂. Studies of HCN inhibition confirmed the random bi-reactant mechanism. HCN was found to be a non-exclusive inhibitor with a binding constant of 0.4 μM.

Methanotrophic bacteria activate and hydroxylate methane to methanol by methane mono-oxygenase in a reaction that requires molecular O₂ as co-substrate and an electron donor for reduction of the second atom of O₂ to water. Methane mono-oxygenase can be found as either a membrane-bound (particulate) or a cytoplasmic (soluble) protein, depending on the growth conditions (Scott *et al.*, 1981; Stanley *et al.*, 1983). NADH is the electron donor for the soluble methane mono-oxygenase from *Methylococcus capsulatus* (Bath) (Colby *et al.*, 1977). Cytochrome *c* was reported to be the electron donor for the particulate methane mono-oxygenase purified from *Methylosinus trichosporium* OB3b (Tonge *et al.*, 1975, 1977), but later experiments indicate that NADH is the electron donor for both the particulate and the soluble methane mono-oxygenase from this organism (Stirling & Dalton, 1979; Scott *et al.*, 1981). Thus at present the most likely reaction catalysed by both the particulate and the soluble methane mono-oxygenase is:



and methane mono-oxygenase can be considered as a ter-reactant enzyme.

The reaction with methane and O₂ *in vivo* has been studied by using a membrane-inlet mass spectrometer for direct measurement of dissolved methane and O₂ in samples of methanotrophic bacteria (Joergensen & Degn, 1983). Methane oxidation at high O₂ concentration followed Michaelis–Menten kinetics with an apparent Michaelis constant of 2 μM for *Ms. trichosporium* and 0.8 μM for strain OU-4-1. This affinity for methane was 10–30 times higher than previous reported values where the methane concentrations were estimated and not directly measured. O₂ utilization by *Ms. trichosporium* at high methane concentrations has also been found to follow Michaelis–Menten kinetics (Joergensen, 1984a). The apparent Michaelis constant was 0.3 μM for O₂, and HCN showed a mixed-type inhibition pattern of both methane and O₂ utilization, indicating a random bi-reactant mechanism for the reaction with methane and O₂, HCN being a non-exclusive inhibitor.

In a reaction catalysed by a multi-reactant enzyme the observed Michaelis constant and turnover number for one substrate will depend on the actual concentrations of the other substrates involved in the reaction. To obtain the true Michaelis constants and information about the reaction sequence it is necessary to perform experiments where the concentration of one substrate is varied while the others are kept at fixed concentrations. A method for keeping the concentration of

methane or O₂ in whole cells at a fixed value is described in the present paper. The technique was used to study the reaction mechanism of methane mono-oxygenase from strain OU-4-1 *in vivo*. A random bi-reactant mechanism for binding of methane and O₂ was found. Binding of one substrate decreased the affinity for the other. HCN was found to be a non-exclusive inhibitor of methane and O₂ binding. These results have been published in a preliminary form elsewhere (Joergensen, 1984b).

Experimental

The isolation and growth conditions of strain OU-4-1, a type II obligate methanotrophic bacterium, has been described previously (Joergensen, 1984b). Cells were grown at 30°C in batch culture in a 1.8-litre fermentor under methane excess. Cells were harvested at cell densities between 200 and 600 mg dry wt./l by centrifugation (5000g for 5 min) and resuspended in a 20 mM-potassium phosphate buffer, pH 7.0, containing 5 mM-MgCl₂ or alternatively directly diluted by the phosphate buffer for the experiments. The experimental sample volume was 5 ml and the temperature was 25°C. The cell dry weight was calculated from the absorbance measured at 550 nm referred to a previously obtained calibration curve.

The open-system technique was used to control the amount of dissolved methane and O₂. The open system consists of a rapidly stirred liquid phase in contact with a continually renewed and controlled gas phase (Degn *et al.*, 1980). The gas phase was controlled by two gas mixers, each consisting of two flow-resistance tubes and a three-way magnetic valve that could switch between the two input lines (with methane and N₂ and with O₂ and N₂ respectively) and in this way regulate the composition of the gas mixture. Methane and O₂ in the gas phase will diffuse into the liquid phase at a rate depending on the gas transfer constant, K , and the gas partial pressure ('tension') of the liquid phase, T_L , and the gas phase, T_G . The consumptions of methane and O₂ by the bacterial suspensions were calculated from:

$$V = K(T_G - T_L) - dT_L/dt \quad (2)$$

The actual concentrations of dissolved gases in the liquid phase were measured by a membrane-inlet mass spectrometer connected to the open-system cuvette. A minicomputer connected to the mass spectrometer calculated the methane- and O₂-utilization rates and regulated the gas mixers. One of the gas mixers was regulated by feedback according to the concentration of dissolved methane or O₂ in the liquid phase. By using this feedback regulation it was possible to keep a pre-

determined content of either methane or O₂ in the sample while the content of the other gas was changed.

The concentrations of the dissolved gases were determined from their solubilities. The solubility used was 1275 μM for O₂ and 1354 μM for methane, both at 0.1 MPa (1 atm) partial pressure and 25°C (Barnes *et al.*, 1976). Methane and O₂ were measured at $m/z = 13$ and $m/z = 32$ respectively.

Gaseous HCN was prepared in a stainless-steel cylinder filled with 0.5 MPa (5 atm) N₂ by combining KCN and H₂SO₄. It was added to the gas phase by a separate gas mixer. The final concentration of HCN in the potassium phosphate buffer equilibrated with the HCN gas was determined by the picric acid method (Hargis, 1978). The solubility of HCN was found to be 5.6 M (20 mM-potassium phosphate buffer, pH 7.0, at 25°C and 0.1 MPa partial pressure).

Results

Methane oxidation by cell suspensions of strain OU-4-1 at high O₂ concentration (> 25 μM) followed Michaelis-Menten kinetics. The apparent K_m for methane was $2.5 \pm 0.9 \mu\text{M}$ and the maximal uptake rate was $70 \pm 15 \text{ nmol of CH}_4/\text{min per mg dry wt.}$ (means \pm S.D. for 12 different batches). The methane uptake at different fixed O₂ concentrations was also measured. Fig. 1 shows an experiment where the O₂ concentration of the sample was kept at 0.1 μM while the methane content of the gas phase was linearly decreased. The methane content of the sample showed a hyperbolic decrease. Double-reciprocal plots of methane uptake and O₂ uptake against methane concentration were constructed. Both plots show straight lines that intersect on the x -axis, indicating a fixed relationship between O₂ uptake and methane uptake at all methane concentrations. The ratio of O₂ uptake to methane uptake was 1.7:1. The deviation from a ratio of 1:1 is due to the further oxidation of methanol, which is either fully oxidized to CO₂ or incorporated into cell material at the level of formaldehyde. The ratio of O₂ uptake to methane uptake can be used for calculation of the growth yield (Joergensen & Degn, 1983). A ratio of 1.7:1 corresponds to a growth yield of 0.4 g/g of methane. Fig. 2 shows double-reciprocal plots of methane uptake against methane concentration for similar experiments at three different O₂ concentrations. The plots show straight lines that intersect in the third quadrant. A replot of reciprocals of maximal methane-uptake rates against reciprocals of O₂ concentrations shows a straight line and gives a K_m value for O₂ of 0.3 μM and a maximal methane-uptake rate of 80 nmol/min per mg dry wt.

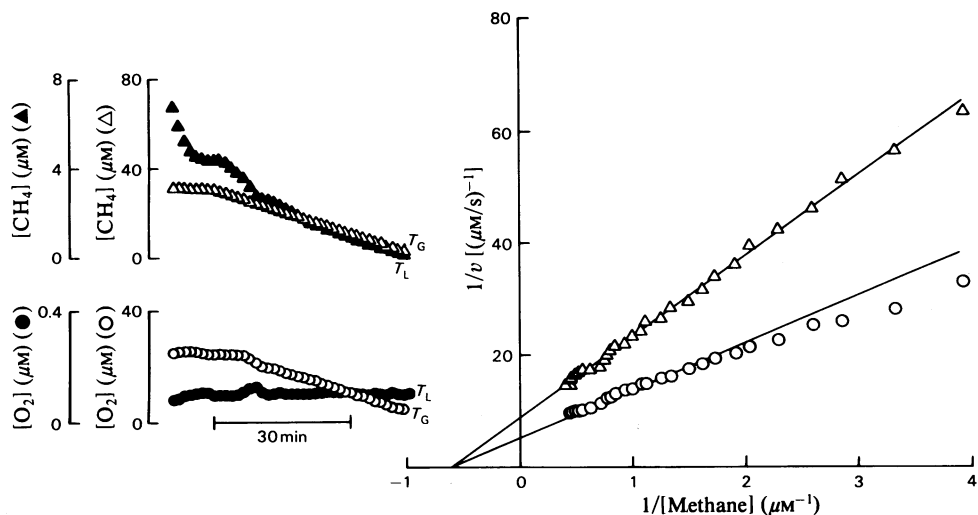


Fig. 1. Methane and O₂ uptake by whole cells of strain OU-4-1 at fixed O₂ concentrations

The O₂ concentration in the sample (\bullet) was kept at 0.1 μM while the methane concentration of the gas phase (\triangle) was linearly decreased. The methane concentration in the sample (\blacktriangle) and the O₂ concentration in the gas phase (\circ) varied as indicated. The double-reciprocal plots show how methane uptake (\triangle) and O₂ uptake (\circ) varied with the methane concentration. T_L , concentration of dissolved gas in the sample; T_G , concentration of gas in the gas phase. The cell content of the sample was 200 mg dry wt./l.

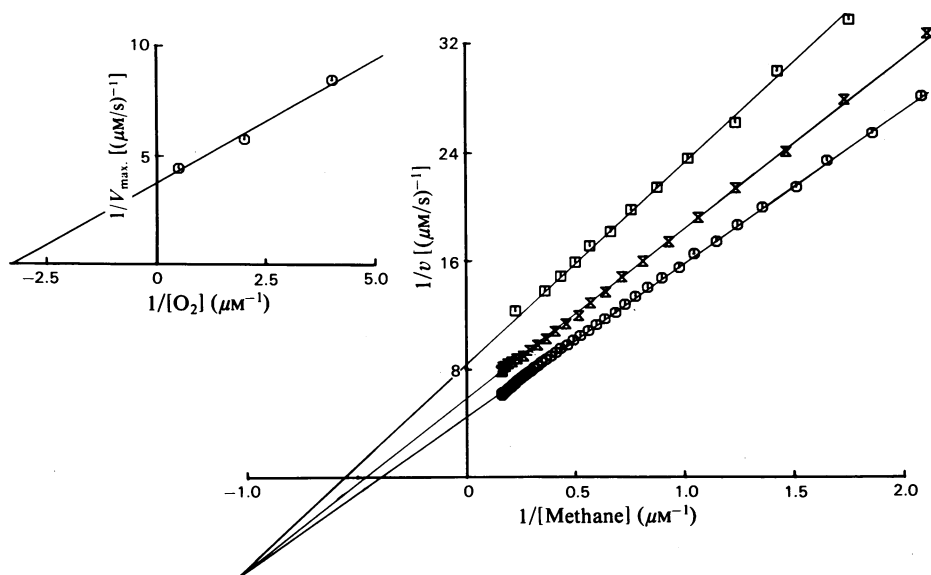


Fig. 2. Double-reciprocal plots of methane uptake by whole cells of strain OU-4-1 at three fixed O₂ concentrations. The O₂ concentrations were 0.25 μM (\square), 0.5 μM (\times) and 2 μM (\circ). Inset: re-plot of intercept against the reciprocal of the O₂ concentration. The cell content of the sample was 200 mg dry wt./l.

O₂ uptake at high methane concentration ($> 50 \mu\text{M}$) followed Michaelis-Menten kinetics with an apparent K_m for O₂ of $0.28 \pm 0.11 \mu\text{M}$ and an apparent V_{max} of $92 \pm 32 \text{ nmol of O}_2/\text{min per mg dry wt.}$ (mean \pm s.d. for 11 different batches).

O₂ uptake at fixed methane concentrations was measured as shown in Fig. 3. The methane concentration in the sample was kept at 1 μM while the O₂ content of the gas phase was decreased linearly with time. The O₂ content of the sample showed a

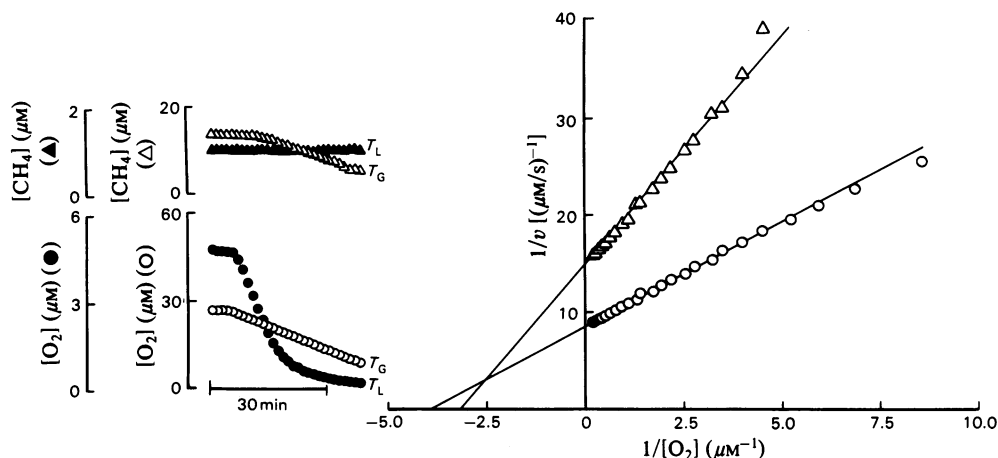


Fig. 3. Methane and O_2 uptake by whole cells of strain *OU-4-1* at fixed methane concentration. The methane concentration in the sample (\blacktriangle) was kept at $1 \mu\text{M}$ while the O_2 concentration of the gas phase (\circ) was linearly decreased. The methane concentration in the gas phase (\triangle) and the O_2 concentration in the sample (\circ) varied as indicated. The double-reciprocal plots show how methane uptake (\triangle) and O_2 uptake (\circ) varied with the O_2 concentration. T_L , concentration of gas in the sample; T_G , concentration of gas in the gas phase. The cell content of the sample was $200 \text{ mg dry wt./l.}$

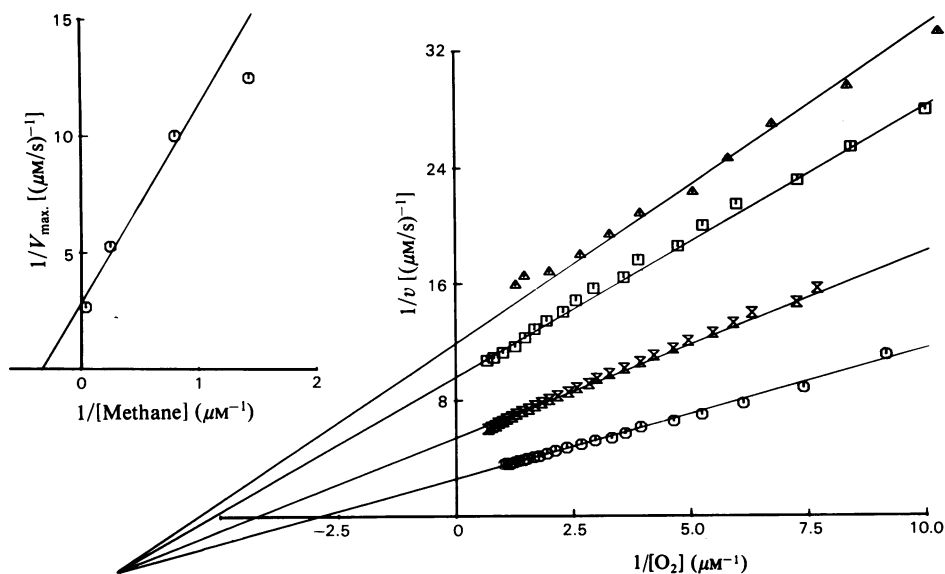


Fig. 4. Double-reciprocal plots of O_2 uptake by whole cells of strain *OU-4-1* at four fixed methane concentrations. The methane concentrations were $0.7 \mu\text{M}$ (\blacktriangle), $1.25 \mu\text{M}$ (\square), $4 \mu\text{M}$ (\otimes) and $50 \mu\text{M}$ (\odot). Inset: re-plot of intercept against the reciprocal of the methane concentration. The cell content of the sample was $200 \text{ mg dry wt./l.}$

hyperbolic decrease. Double-reciprocal plots of methane uptake and O_2 uptake against O_2 concentration were constructed. Both plots show straight lines that intersect near the x -axis. This indicates a constant relationship between methane uptake and O_2 uptake for all O_2 concentrations. The ratio

of O_2 uptake to methane uptake was 1.7:1. Fig. 4 shows double-reciprocal plots of O_2 uptake against O_2 concentration for similar experiments at four different methane concentrations. The plots all show straight lines that intersect in the third quadrant. A replot of reciprocals of maximal rates

against reciprocals of methane concentrations gives a K_m value for methane of $3 \mu\text{M}$ and a maximal O₂-uptake rate of $115 \text{ nmol/min per mg dry wt.}$

The reaction pattern seen in Figs. 2 and 4 can be explained by a system where the two substrates bind randomly to methane mono-oxygenase and the binding of one substrate decreases the affinity for the other substrate (Segel, 1975). The decrease in affinity for the second substrate due to binding of the first substrate is given by the factor α and can be calculated from $1/V_{\text{max.}}(1-\alpha) = y$ -values of intersect. $1/K_m$ is equal to the x -value of intersect. The values of α , K_m and $V_{\text{max.}}$ obtained from Figs. 2 and 4 are given in Table 1.

HCN was found to inhibit methane uptake and O₂ uptake. The effect on methane uptake was studied at saturating concentrations of O₂. Fig. 5 shows double-reciprocal plots of methane uptake at five different concentrations of HCN. The plots show straight lines that intersect in the third quadrant, resulting in a pattern characteristic for a

mixed-type inhibition. The inhibitory constants, K_{ii} and K_{is} , obtained from intercept and slope replots are $0.7 \mu\text{M}$ and $3 \mu\text{M}$ respectively. Fig. 6 shows the effect of HCN on O₂ uptake at saturating concentrations of methane. The double-reciprocal plots of O₂ uptake at five different HCN concentrations are linear and intersect in the second quadrant, showing a mixed-type inhibition pattern. The inhibitory constants obtained from intercept and slope replots are $0.7 \mu\text{M}$ and $0.1 \mu\text{M}$ respectively. This pattern for the HCN inhibition is in agreement with a random bi-reactant reaction mechanism for binding of methane and O₂ to methane mono-oxygenase, cyanide being a non-exclusive inhibitor of both substrates. According to the nomenclature given by Segel (1975), the interaction between cyanide and methane binding can be expressed by the factor γ and the interaction between cyanide and O₂ binding can be expressed by the factor β . The slope inhibition constant, K_{is} , equals βK_i for cyanide inhibition of methane uptake at saturating O₂ concentration and γK_i

Table 1. Kinetic constants for methane and O₂ binding by whole cells of strain OU-4-1

The data were obtained from Figs. 2 and 4 in accordance with the kinetic pattern of a bi-reactant enzyme as described by Segel (1975).

Fixed substrate	α	$K_m(\text{O}_2)$ (μM)	$\alpha K_m(\text{O}_2)$ (μM)	$V_{\text{max.}}(\text{O}_2)$ (nmol of O ₂ /min per mg dry wt.)	$K_m(\text{CH}_4)$ (μM)	$\alpha K_m(\text{CH}_4)$ (μM)	$V_{\text{max.}}(\text{CH}_4)$ (nmol of CH ₄ /min per mg dry wt.)
O ₂ (Fig. 2)	2.6	—	0.3	—	1	2.6*	80
Methane (Fig. 4)	2.5	0.14	0.35*	115	—	3	—

* Calculated from α and K_m .

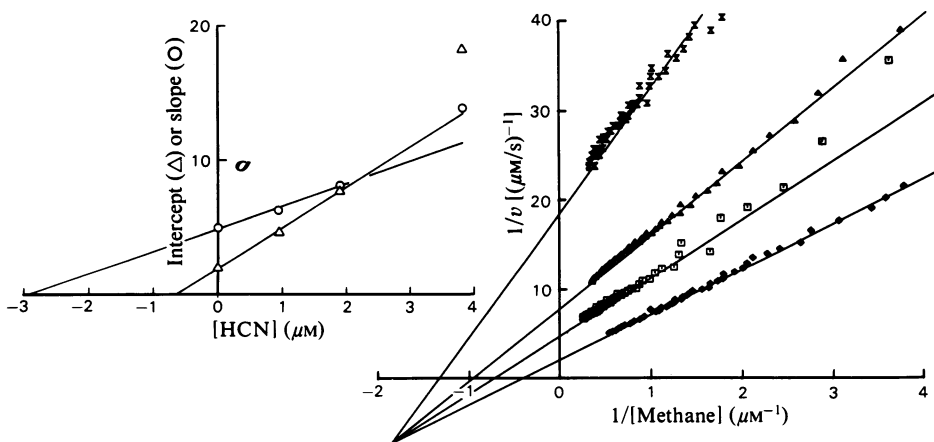


Fig. 5. HCN inhibition of methane uptake by whole cells of strain OU-4-1

Double-reciprocal plots and secondary plots for four different HCN concentrations: $0 \mu\text{M}$ (\diamond), $0.95 \mu\text{M}$ (\square), $1.9 \mu\text{M}$ (\blacktriangle) and $3.8 \mu\text{M}$ (\otimes). The O₂ concentration was kept above $50 \mu\text{M}$. The cell content of the sample was $400 \text{ mg dry wt./l.}$

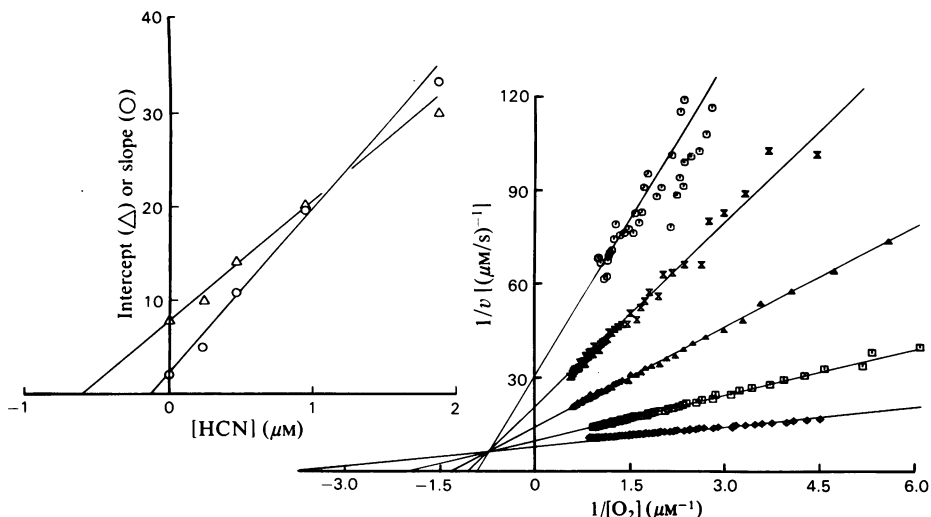


Fig. 6. HCN inhibition of O_2 uptake by whole cells of strain OU-4-1. Double-reciprocal plots and secondary plots for five different HCN concentrations: $0 \mu\text{M}$ (\diamond), $0.24 \mu\text{M}$ (\square), $0.47 \mu\text{M}$ (\blacktriangle), $0.94 \mu\text{M}$ (\otimes) and $1.88 \mu\text{M}$ (\odot). The methane concentration was kept above $50 \mu\text{M}$. The cell content of the sample was 75 mg dry wt./l .

Table 2. Kinetic constants for cyanide inhibition of O_2 and methane uptake by whole cells of strain OU-4-1. The data were obtained from Figs. 5 and 6.

Re-plot type ...	Intercept (K_{ii})	Slope (K_{is})	
		γK_i (μM)	βK_i (μM)
Inhibitor constant ...	$\beta\gamma K_i$ (μM)		
Methane uptake (Fig. 5)	0.7	—	3.0
O_2 uptake (Fig. 6)	0.7	0.1	—

for cyanide inhibition of O_2 uptake at saturating methane concentration. The intercept inhibition constant, K_{ii} , equals $\beta\gamma K_i$ in both cases and has to be the same for cyanide inhibition of both methane uptake and O_2 uptake. The experimental values for K_{ii} fulfilled this requirement within the accuracy of the measurements. The inhibition constants are given in Table 2. K_i , β and γ were calculated from these data to be $0.43 \mu\text{M-HCN}$, 7 and 0.23 respectively.

Discussion

The methane mono-oxygenase from strain OU-4-1 was membrane-bound, from the growth conditions, the existence of internal membranes and the inhibition by HCN (Joergensen, 1984b). It has been shown to be the rate-limiting enzyme in methane oxidation by *Ms. trichosporium* (Joergensen, 1984a) and strain OU-4-1 (Joergensen, 1984b). This might be expected, as methane mono-oxygenase is the only energy-

requiring enzyme participating in methane oxidation. It requires an electron donor, probably NADH, for activity. Its product, methanol, is further oxidized to formaldehyde by an NAD-independent methanol dehydrogenase, which delivers its electrons to the respiratory chain at the level of cytochrome *c* (Duine & Frank, 1981). Formaldehyde is either assimilated into cell material or fully oxidized via formate to CO_2 . NAD-dependent formaldehyde dehydrogenases and formate dehydrogenases have been found in methanotrophs (Zatman, 1981), and the final steps in oxidation of methane to CO_2 can thus provide NADH for the initial activation of methane. Methanol cannot serve as an electron donor for methane mono-oxygenase unless either a form of reversed electron flow or an NADH-independent methane mono-oxygenase exists. Methane mono-oxygenase activity has been stimulated by oxidation of C_2 to C_4 primary alcohols, which do not produce NADH directly, and this may be due to a form of reversed electron flow (Leak & Dalton, 1983).

The reaction mechanism of methane mono-oxygenase was simplified to a bi-reactant enzyme system. This simplification will only hold as long as the NADH concentration stays either constant or above its saturation level. The fact that I got straight double-reciprocal plots indicates that this requirement was fulfilled. To obtain more information about the role of NADH in the enzyme reaction it is necessary to be able to control the NADH concentration simultaneously with methane and O₂. This will only be possible in cell-free extracts. Unfortunately it has not yet been possible to make a stable cell-free preparation of methane mono-oxygenase from strain OU-4-1. The reaction mechanism of methane mono-oxygenase in whole cells was found to fit a random bi-reactant system where the binding of one substrate decreased the affinity for the other. The reason for the decrease in affinity for the second substrate after binding of the first may be that the two binding sites are so close that binding of one substrate spatially hindered binding of the other.

HCN was a potent inhibitor of methane and O₂ uptake by strain OU-4-1. HCN may inhibit several enzymes in whole cells. It has been shown to inhibit the particulate methane mono-oxygenase from *Mc. capsulatus* (Bath) (Stanley *et al.*, 1983) and from *Ms. trichosporium* OB3b (Tonge *et al.*, 1977) and methanol dehydrogenase from *Hyphomicrobium* X, a facultative methylotrophic bacterium (Duine & Frank, 1980). HCN inhibited O₂ uptake with a K_i value of about 1 μM when methanol or formaldehyde was oxidized by whole cells of strain OU-4-1 (results not shown). The inhibition pattern was similar for methanol oxidation and formaldehyde oxidation. This indicates that the observed effect of HCN was due to inhibition of the terminal oxidase, a cytochrome *aa*₃, rather than to inhibition of methanol dehydrogenase. The low K_i supports this view, as the K_i for HCN inhibition of methanol dehydrogenase from *Hyphomicrobium* X has been found to be 1 mM (Duine & Frank, 1980). HCN caused a mixed-type inhibition of O₂ uptake when methane was oxidized by strain OU-4-1, with a slope inhibition constant of 0.1 μM and an intercept inhibition constant of 0.7 μM (Fig. 6). The effect of HCN in this case was probably entirely due to inhibition of methane mono-oxygenase, since the inhibition constants were lower than that found when methanol was oxidized and since methane uptake at high O₂ concentration also was inhibited by very low HCN concentrations (Fig. 5). However, an effect of HCN on the further oxidation of methane to CO₂ and thereby on the formation of NADH cannot be ruled out. A change in the NADH concentration may affect the methane mono-oxygenase reaction, as discussed above. To verify the

effect of HCN, it is preferable to repeat the experiments with a cell-free preparation of methane mono-oxygenase under controlled NADH concentration. Assuming that the effect of HCN on strain OU-4-1 oxidizing methane was entirely due to inhibition of methane mono-oxygenase, the observed inhibition pattern confirmed the random binding of methane and O₂. HCN is then a non-exclusive inhibitor, indicating that HCN, methane and O₂ bind at different sites on methane mono-oxygenase. HCN decreased the apparent K_m for methane and increased the apparent K_m for O₂. This can be explained by a mechanism in which cyanide spatially or in some other way interacts with the O₂ binding and thereby increases the apparent K_m for O₂. The decrease in apparent K_m for methane may be caused by the effect of HCN on the O₂ binding. The apparent K_m for methane increases 2.6-fold when O₂ binds to methane mono-oxygenase (Table 1). HCN inhibition may reverse this effect of O₂, and an apparent decrease in K_m for methane results.

In conclusion, the binding of methane and O₂ to methane mono-oxygenase follows a random order. Binding of one substrate decrease the affinity for the other, suggesting that the binding sites are very close. HCN inhibits methane and O₂ binding in a non-exclusive way. It decreases the affinity for O₂ but increases the affinity for methane, indicating an interaction with the O₂-binding site. Investigations into the role of NADH will have to await the preparation of stable cell-free extracts of methane mono-oxygenase.

I am grateful to Dr. Hans Degn for his advice and encouragement and to Professor Howard Dalton for discussions of the manuscript. This work was supported by the Danish Science Research Council (Grant 113495).

References

- Barnes, L. J., Drozd, J. W., Harrison, D. E. F. & Hamer, G. (1976) in *Microbial Production and Utilization of Gases (H₂, CH₄, CO)* (Schlegel, H. G., Gottschalk, G. & Pfennig, N., eds.), pp. 389–402, E. Goltze K.G., Göttingen
- Colby, J., Stirling, D. I. & Dalton, H. (1977) *Biochem. J.* **165**, 395–402
- Degn, H., Lundsgaard, J. S., Petersen, L. C. & Ormicki, A. (1980) *Methods Biochem. Anal.* **26**, 47–77
- Duine, J. A. & Frank, J. (1980) *Biochem. J.* **187**, 213–219
- Duine, J. A. & Frank, J. (1981) in *Microbial Growth on C₁ Compounds* (Dalton, H., ed.), pp. 31–41, Heyden, London
- Hargis, L. G. (1978) in *Colorimetric Determination of Non-Metals* (Boltz, O. F. & Howell, J. A., eds.), pp. 68–78, John Wiley and Sons, New York
- Joergensen, L. (1984a) in *Microbial Gas Metabolism: Metabolic and Biotechnological Aspects* (Poole, R. K. & Dow, C. S., eds.), Academic Press, New York, in the press

- Joergensen, L. (1984b) in *Gas Enzymology* (Degn, H., Cox, R. P. & Toftlund, H., eds.), Reidel, Dordrecht, in the press
- Joergensen, L. & Degn, H. (1983) *FEMS Microbiol. Lett.* **20**, 331-335
- Leak, D. J. & Dalton, H. (1983) *J. Gen. Microbiol.* **129**, 3487-3497
- Scott, D., Brannan, J. & Higgins, I. J. (1981) *J. Gen. Microbiol.* **125**, 63-72
- Segel, I. H. (1975) *Enzyme Kinetics: Behaviour and Analysis of Rapid Equilibrium and Steady-State Enzyme Systems*, pp. 273-299, John Wiley and Sons, New York
- Stanley, S. H., Prior, S. D., Leak, D. J. & Dalton, H. (1983) *Biotechnol. Lett.* **5**, 487-492
- Stirling, D. I. & Dalton, H. (1979) *Eur. J. Biochem.* **96**, 205-221
- Tonge, G. M., Harrison, D. E. F., Knowles, C. J. & Higgins, I. J. (1975) *FEBS Lett.* **58**, 293-299
- Tonge, G. M., Harrison, D. E. F. & Higgins, I. J. (1977) *Biochem. J.* **161**, 333-344
- Zatman, L. J. (1981) in *Microbial Growth on C₁ Compounds* (Dalton, H., ed.), pp. 42-54, Heyden, London